Hindawi Publishing Corporation
International Journal of Distributed Sensor Networks
Volume 2012, Article ID 685054, 13 pages
doi:10.1155/2012/685054

Research Article

Distributed Strain Sensor Networks for In-Construction Monitoring and Safety Evaluation of a High-Rise Building

X. W. Ye, Y. Q. Ni, and Y. X. Xia

Department of Civil and Environmental Engineering, The Hong Kong Polytechnic University, Hung Hom, Kowloon, Hong Kong

Correspondence should be addressed to Y. Q. Ni, ceyqni@polyu.edu.hk

Received 14 July 2012; Accepted 9 August 2012

Academic Editor: Ting-Hua YI

The New Headquarters of Shenzhen Stock Exchange (NHSSE), currently being constructed in Shenzhen, China, is a high-rise building with a height of 245 m. One salient feature of NHSSE is its huge floating platform with an overall plan dimension of 98 m× 162 m and a total height of 24 m, making it one of the largest cantilever structures in the world. In recognition of the uniqueness of the floating platform, a long-term structural health monitoring (SHM) system has been designed and implemented by The Hong Kong Polytechnic University for both in-construction and in-service monitoring of NHSSE. As part of this monitoring system, 224 vibrating-wire strain gauges have been permanently installed to measure the strain responses of key structural components of the floating platform. A wireless strain monitoring system by integrating local tethered data acquisition and long-range wireless data transmission has been developed for real-time strain monitoring and visualization. This paper presents the stress evolution of the floating platform during dismantlement of temporary supports on the basis of the real-time monitoring data and the statistical stress analysis and safety evaluation of the floating platform by use of the long-term monitoring data, as well as the effect of the welding residual stress on structural safety of NHSSE.

1. Introduction

Structural health monitoring (SHM) of building structures, especially for super-tall buildings and out-of-codes buildings, has been a cutting-edge technology and gained more and more attention in civil engineering community over the past decade [1–5]. With the increasing complexity of modern building structures, civil engineers have met a challenging task of ensuring not only the life-cycle safety of these building structures but also their robustness in resisting natural and/or man-made hazards such as earthquakes, typhoons, and fires, and so forth at both in-construction and in-service stages. Instrumented high-rise buildings with long-term SHM systems are able to provide the most authentic and practical information for real-time assessment of structural integrity, durability, and reliability as well as for decision-making on structural inspection and maintenance actions. A recent application of the SHM technology to high-rise buildings is the Canton Tower permanently instrumented with more than 700 sensors of sixteen types which were installed in parallel with the construction progress leading to a life-cycle monitoring architecture [6–9].

In the applications of SHM to building structures, static and/or dynamic strain monitoring of key structural components is essential since strain measurement data after being transferred into the corresponding stress data can be directly used to indicate the utilization extent of the resistance of materials as well as the safety margin or reliability of the structural components. The physical quantities of acceleration, moment, and torque also can be derived through careful design and implementation of densely distributed strain sensor networks on the targeted building structure, and further for data-driven health and safety condition evaluation. Additionally, several investigations demonstrate that strain measurement as a local structural response shall be more suitable for local behavior characterization or damage detection than vibration-based acceleration data. Real-world practice of strain monitoring of large-scale structures by use of electrical strain gauges, vibrating-wire strain gauges, or fiber optical strain sensors has been widely reported [10–12], and research efforts devoted to strain-based condition assessment of instrumented structures have been made by different investigators [13–19].

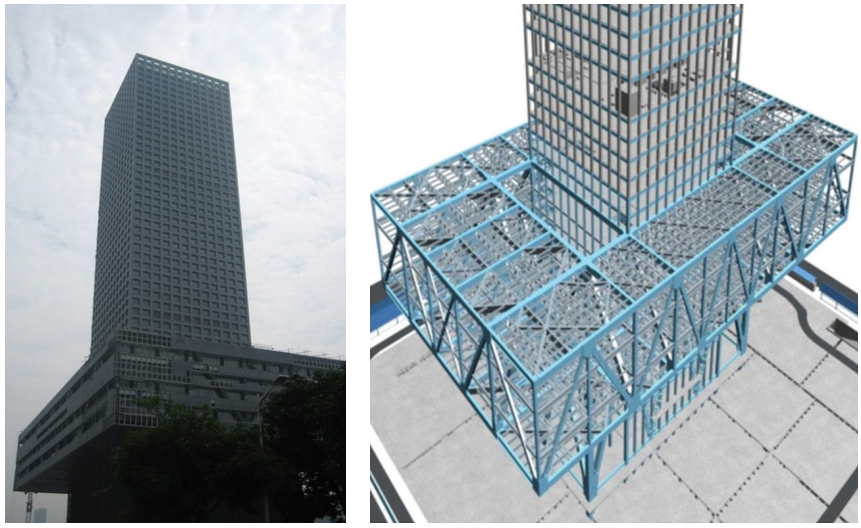

(a) (b)

Figure 1: New Headquarters of Shenzhen Stock Exchange (NHSSE).

The New Headquarters of Shenzhen Stock Exchange (NHSSE), which is planned as a financial center in Shenzhen, China, is a high-rise building with a height of 245 m. Its surrounding area is designed as a public space for festivals and gatherings, while the main tower will serve for various functions including trading floor, Shenzhen Stock Exchange offices, and so forth. A salient feature of this building exists in its huge floating platform, which is one of the largest cantilever structures in the world. In view of this uniqueness and the importance of NHSSE, a long-term SHM system has been devised and implemented by The Hong Kong Polytechnic University to continuously monitor the structural responses (strain, temperature, displacement, and acceleration) of the floating platform during its whole life cycle, including both construction and service stages [20]. This paper explores several key issues in developing and implementing distributed strain sensor networks on the floating platform commencing from its construction stage for long-term strain monitoring in real time and presents the statistical stress analysis and safety evaluation of the floating platform using the long-term strain monitoring data.

2. NHSSE and Its SHM System

2.1. New Headquarters of Shenzhen Stock Exchange (NHSSE). As illustrated in Figure 1, the New Headquarters of Shenzhen Stock Exchange (NHSSE), with 46 storeys above the ground and 3 basement storeys, is composed of 4 segments in the vertical direction of the building. The first segment is the reinforced concrete basement storeys. The second segment, with a rectangular cross-section of 54 m × 90 m, is a trussed tube structure from the 1st floor to the 6th floor of the main tower. The floating platform, from the 7th floor to the 10th floor of the building, constitutes the third segment with a rectangular plan of 98 m × 162 m. From the 10th floor of the main tower above, the fourth segment of the building is a tube-in-tube structure consisting of an inner reinforced concrete core and an outer shaped steel and reinforced concrete composite frame. The inner structure has a rectangular cross-section of 28 m × 32 m, and the outer structure has a 54 m × 54 m square cross-section.

As the most distinct feature of NHSSE, the huge floating platform is a mega-overhanging steel truss structure with a total height of 24 m. The floating platform consists of 14 crisscrossed steel trusses which are divided into 6 types. The main truss structures are assembled by lots of welded composite joints made of box-sectional members. The outrigger truss storeys have the outrigger components of 22 m in the south-north direction and 36 m in the east-west direction at a height of 36 m above the ground, which makes the floating platform one of the largest cantilever structures in the world.

2.2. SHM System for NHSSE. In recognizing the uniqueness of the floating platform, a long-term SHM system was designed and implemented by The Hong Kong Polytechnic University to monitor the structural responses (strain, temperature, displacement, and acceleration) of the cantilever trusses of NHSSE in both construction and service stages. The SHM system for NHSSE consists of six modules: Module 1—Sensory System (SS), Module 2—Data Acquisition and Transmission System (DATS), Module 3—Data Processing and Control System (DPCS), Module 4—Data Management System (DMS), Module 5—Structural Health Evaluation System (SHES), and Module 6—Inspection and Maintenance System (IMS). The integration of these six modules is shown in Figure 2. The SS and DATS are located in the structure, the DPCS, DMS, and SHES are inside the monitoring center room, and the IMS is a portable system.

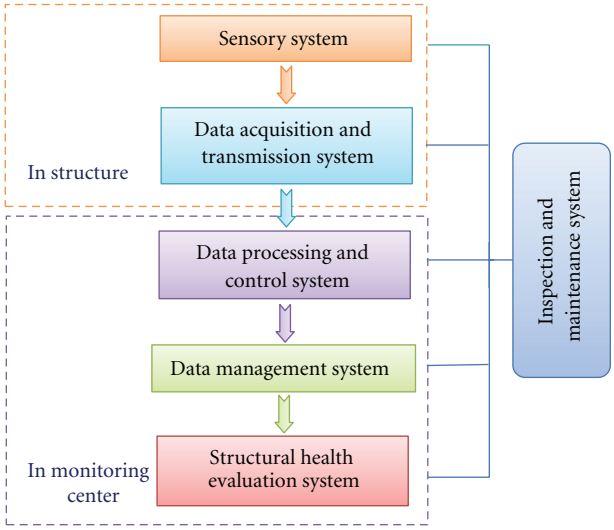

Figure 2: Modular architecture of SHM system for NHSSE.

The SS system includes vibrating-wire strain gauges, temperature sensors, accelerometers, and a vision-based displacement tracking system. In this SHM system, the vibrating-wire strain gauge was adopted for strain measurement due to its advantage of antielectromagnetic interference in comparison with the electrical strain gauge, and its merit of cost-effectiveness compared with the fiber optical strain sensor. The Geokon Model 4000 vibrating-wire strain gauge was used to measure the strain and temperature simultaneously. With the measured temperature data, the strain data could be calibrated by taking into account the temperature effect on the resonant frequency of the tensioned steel wire of the vibrating-wire strain gauge. The DATS system is composed of 4 stand-alone data acquisition units (DAUs) and 2 wireless LAN bridges for data transmission in construction stage. The 4 DAUs are assigned at the 4 weak electricity wells which are located in the four corners of the core structure. They are used to collect the signals from the surrounding sensors, digitize the analogue signals, and wirelessly transmit the data into the central room. The DPCS comprises high-performance servers and data-processing software. This system is used for routine data processing, structural and system status monitoring and prewarning as well as display of the data. The DMS consists of a high-performance server, relational Oracle-based database system and geographic information system- (GIS-) based data management software. The SHES is composed of a high-performance server and structural health evaluation software. It is used for processing and analyzing the monitoring data and evaluating and diagnosing the structural condition. It emphasizes on control-oriented evaluation of structural status in construction stage and updating of the finite element model (FEM) for the purpose of structural damage detection. The IMS is a laptop-computer-aided portable system for inspecting and maintaining sensors, DAUs, and cabling networks.

3. Distributed Strain Sensor Networks

3.1. Deployment Sections of Strain Gauges. The structural strains of the cantilever trusses of NHSSE are of the utmost concern at the construction stage, especially during temporary supports' dismantlement of the floating platform. After examining the load transfer mechanism and load-carrying characteristics of the cantilever trusses of NHSSE, 56 critical cross-sections on key structural members of the cantilever trusses have been selected for strain monitoring and further stress analysis. All the instrumented cross sections are allocated on the upper chords, diagonal struts, and bottom chords of four main steel trusses (TR1, TR2, TR4, and TR5) and the internal diagonal bracings on the 7th floor, which are bisymmetrically distributed on the floating platform, as illustrated in Figure 3. The deployment sections of strain gauges are divided into four monitoring zones, that is, southeast zone, southwest zone, northeast zone, and northwest zone. Each monitoring zone contains 14 instrumented sections and each instrumented section has 4 vibrating-wire strain gauges. As a result, a total of 224 vibrating-wire strain gauges have been permanently installed on the floating platform. The strain sensor networks distributed in the northeast zone of the floating platform are illustrated in Figure 3 (the instrumented section number 6 is located at the diagonal bracing out of the floating platform and the instrumented section number 14 is located at the internal diagonal bracing on the 7th floor of the floating platform). Figure 4 shows the sectional view of the deployment sections of strain gauges on four main trusses and the diagonal bracings on the 7th floor of the floating platform.

3.2. Deployment Locations of Strain Gauges. The strain gauges are deployed in consideration of the type of cross-sections (rectangle or I section), loading kinds (axial force, bending or bidirectional bending, etc.), and limitations due to construction and inaccessibility. As illustrated in Figure 5, four vibrating-wire strain gauges are installed on the two webs and the bottom flange of the upper chords (the instrumented sections number 2, 3, 8, and 11), bottom chords (the instrumented sections number 4, 5, 10, and 13), and the internal diagonal bracings on the 7th floor (the instrumented section number 14). Four vibrating-wire strain gauges are installed on four surfaces of the diagonal struts (the instrumented sections number 6, 7, 9, and 12) and the corner columns (the instrumented section number 1). In Figure 5, the location of each strain gauge is denoted as "$n-m(o)$" where n stands for the instrumented section, m is the sensor number, and o indicates the sensor orientation.

3.3. Real-Time Monitoring and Wireless Transmission. The measuring principle of a vibrating-wire strain gauge relies on the relationship between the resonant frequency of the tensioned steel wire and the strain of the targeted structure. The frequency output of the vibrating-wire strain gauge is immune to electrical noise and is capable of signal transmission of several kilometers without loss of signal. Therefore, the vibrating-wire strain gauge has been the

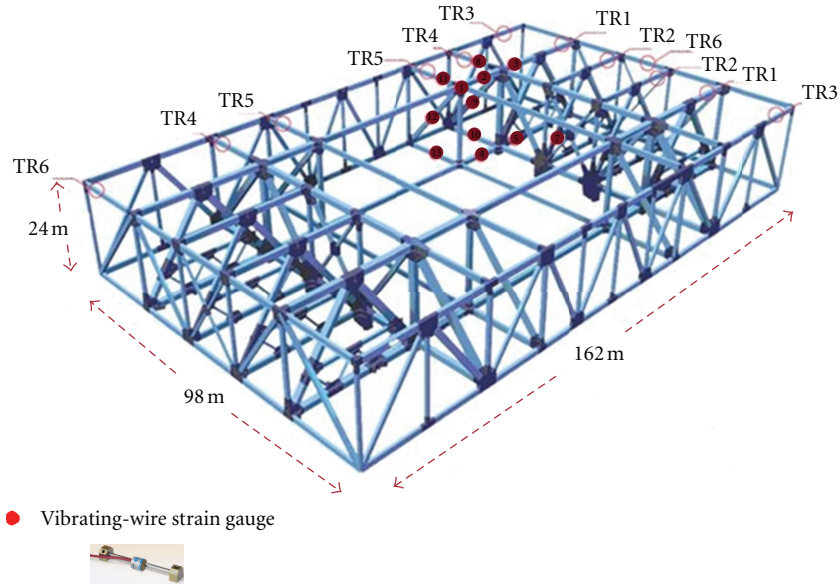

Figure 3: Deployment sections of strain gauges on floating platform.

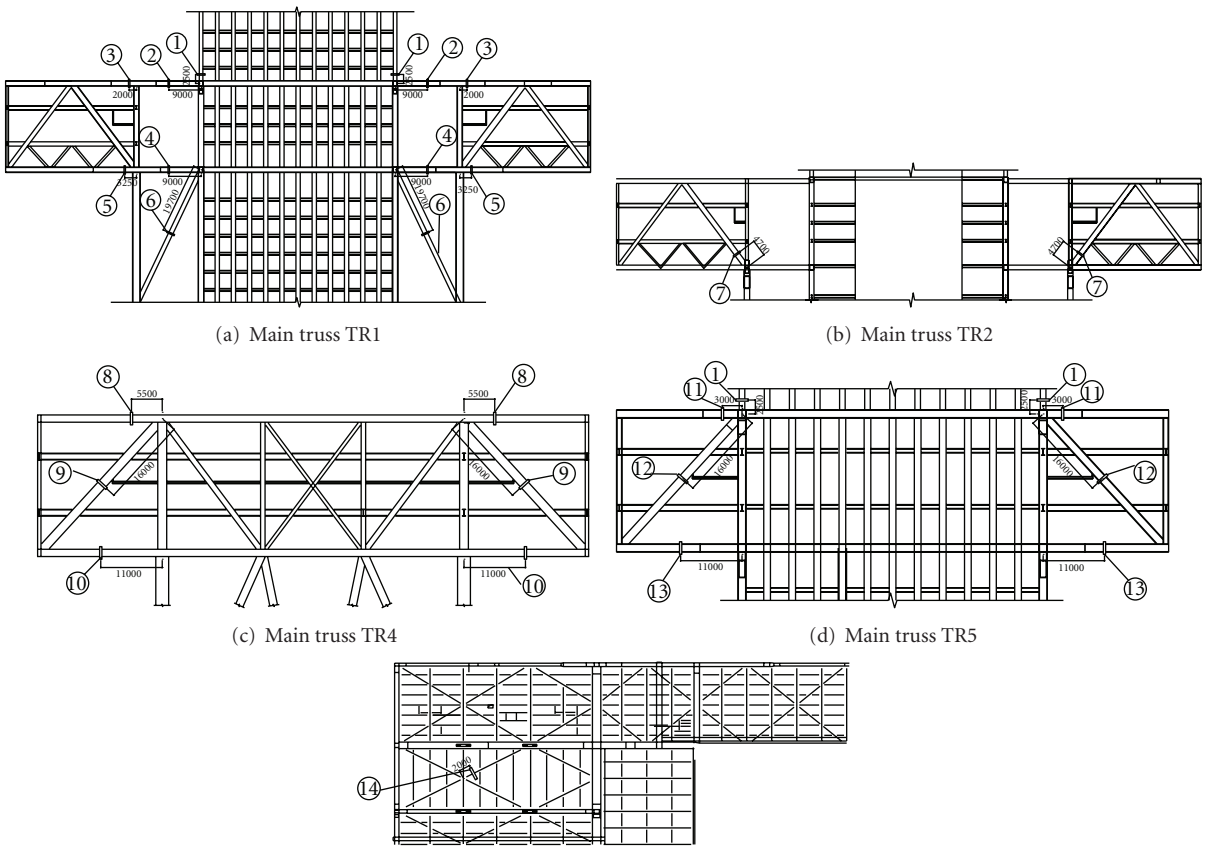

(a) Main truss TR1

(b) Main truss TR2

(c) Main truss TR4

(d) Main truss TR5

(e) Diagonal bracings on the 7th floor of floating platform

Figure 4: Sectional view of deployment sections of strain gauges.

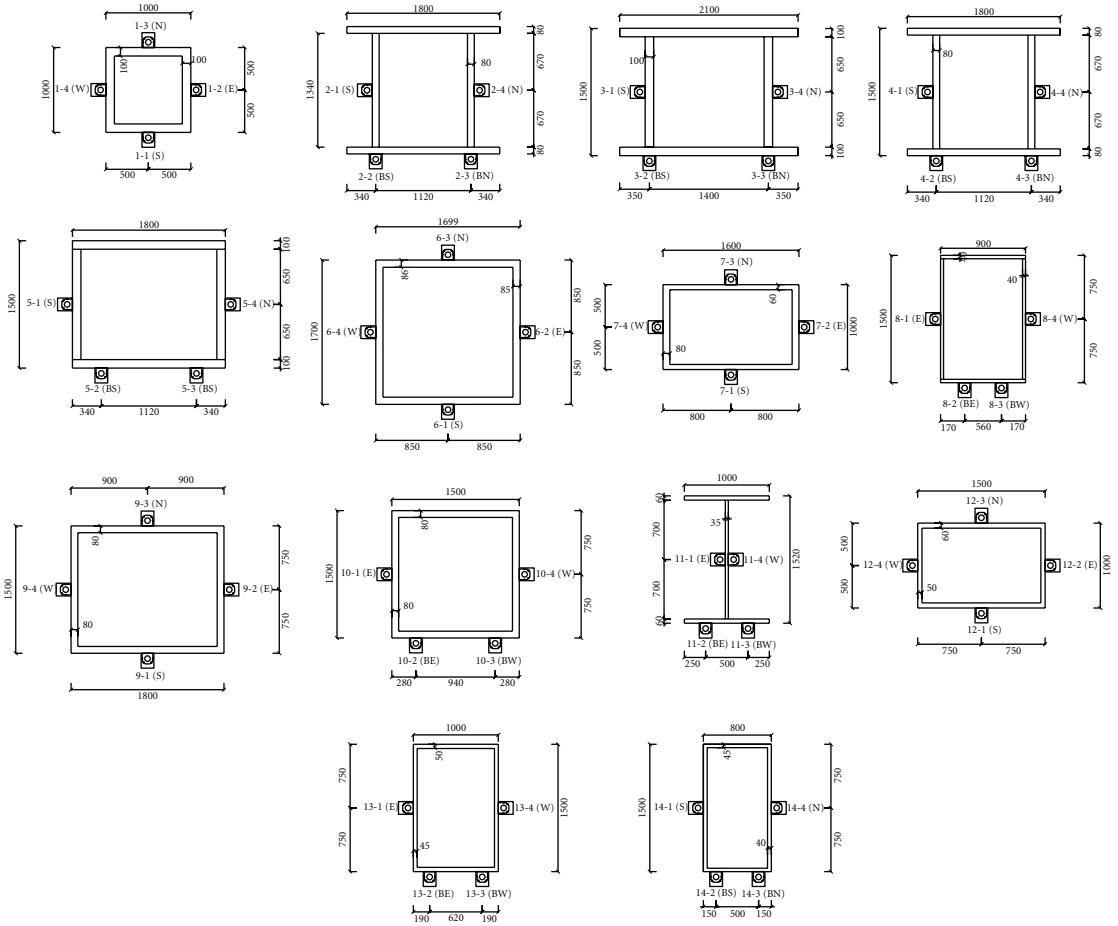

Figure 5: Deployment locations of strain gauges on instrumented sections.

(a) (b)

Figure 6: Installation and protection of strain gauges.

most common type of strain gauges being widely used for long-term static strain monitoring of large-span or high-rise civil infrastructure. In many applications, especially during in-construction stage, the robustness and effectiveness of the protective measures for the vibrating-wire strain gauges and signal transmission cables are essential to the success of a long-term strain monitoring system. In this project, all the vibrating-wire strain gauges and their cabling networks are protected by stainless steel covers which are screwed onto the surfaces of the steel truss members and sealed with a sealant to prevent water seeping into the sensor housings, as illustrated in Figure 6. By these means, the survival rate of the vibrating-wire strain gauges in this project reaches to 96.88% (only 7 out of 244 vibrating-wire strain gauges were damaged in construction stage).

(a) (b)

Figure 7: Wireless data acquisition and transmission system.

The sampling rate for each vibrating-wire strain gauge is set as one data per second in the process of dismantling the temporary supports and switches to one data per 90 seconds in normal service circumstance. It can be adjusted as required for different purposes. The signals from the vibrating-wire strain gauges are first transmitted to the data loggers inside the structure through coaxial wires and then sent to the server PC at a site office (outside the in-construction building) in a wireless way through a pair of wireless access points (2 wireless LAN bridges) for real-time monitoring in construction stage (refer to Figure 7). By doing so, the strain is real-time monitored and visualized remotely thus greatly facilitating the in-construction monitoring and control. For instance, this wireless real-time monitoring system has played an important role in instructing dismantlement of the temporary supports of the floating platform (will be discussed in details in Section 4).

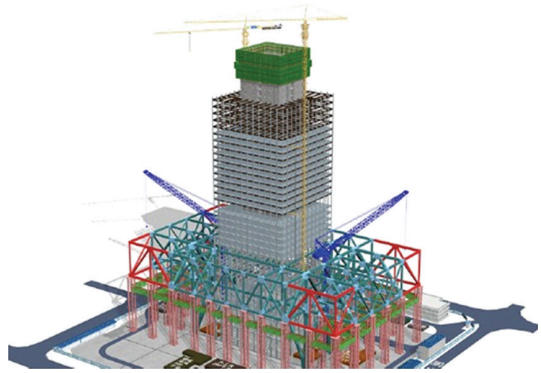

Figure 8: Skeleton diagram of floating platform erection.

4. Strain Monitoring during Dismantlement of Temporary Supports

4.1. Unloading Process of Temporary Supports. During the erection of the floating platform, tower cranes were used to hoist the steel framework, and a temporary brace-frame structure was used to support the cantilever trusses. As illustrated in Figure 8, two-tier connecting trusses were added to strengthen the temporary supports and ensure the transversal stability. After completing the erection of the floating platform, the temporary supports were dismantled by use of the sandbox unloading technology. A rational planning for the unloading process is deemed to be extremely significant because (i) the total weight of the cantilever trusses for unloading is up to 9,473 tons, and it is required to make each control point subside uniformly and synchronously to ensure the consistent deformation of the floating platform and main tower; (ii) there are in total 46 widespread temporary supports for unloading; therefore, it is necessary to carry out the dismantling work in a well-coordinated way; (iii) the minimum supporting force is about 102 tons, while the maximum one is around 305 tons.

Recognizing the above, a stage-by-stage procedure for unloading temporary supports in batches was formulated to make the transition of the structural stress and configuration in a steady and successive way. The temporary supports were divided into 3 groups, that is, TJO, TJM, and TJI as illustrated in Figure 9. The unloading sequence of the temporary supports was from the outer positions (TJO), through middle positions (TJM), to the inner positions (TJI), and each step was executed simultaneously to prevent uneven deformation. A new structural system was generated upon the completion of dismantlement of all temporary supports. During the unloading process of the temporary supports, the SHM system is highly desirable to detect the potential anomaly such as sudden significant rising of the structural stress, and the unloading work would be suspended once such anomaly happens.

Table 1: Statistics of the maximum stress increments and strength utilization factors during dismantlement of temporary supports.

Monitoring zone	Tensile stress increment (MPa)	SUF	Sensor location	Compressive stress increment (MPa)	SUF	Sensor location
Southeast (SE)	20.03	6.8%	2-1 (S)	21.42	7.3%	4–2 (BS)
Southwest (SW)	19.65	6.7%	2-2 (BS)	18.73	6.3%	7–4 (W)
Northeast (NE)	18.59	6.3%	2–4 (N)	21.02	7.1%	4-3 (BN)
Northwest (NW)	19.27	6.5%	2-3 (BN)	19.23	6.5%	4-3 (BN)

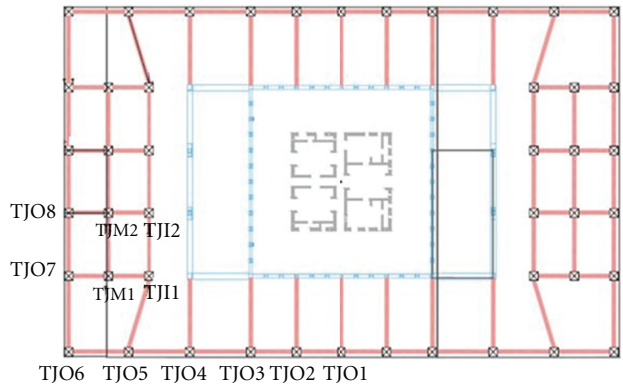

Figure 9: Layout of temporary supports.

4.2. Statistical Analysis of Monitoring Data. The temporary supports were dismantled step by step (commences at 09:00 am on 3 April 2010 and ends at 16:00 pm on 3 April 2010), with the unloading weight being small at the beginning and getting larger and larger till the temporary supports were totally disconnected with the cantilever trusses. The strain data from all the deployed vibration-wire strain gauges were real-time measured during dismantlement of the temporary supports and wirelessly transmitted to the site office for visualization. The stress increments of all the instrumented structural components were automatically derived by simply multiplying the measured strain increments by the elastic modulus of steel in assumption of elastic strain. The strength utilization factor (SUF), which is defined as the ratio of the stress increment of each instrumented structural component to the design strength of steel (295 MPa in this case), was also obtained using the following formula:

$$\text{SUF} = \frac{\Delta s}{f_{\text{sd}}}, \tag{1}$$

where SUF is the strength utilization factor; Δs is the stress increment of each instrumented structural component; f_{sd} is the design strength of steel.

Table 1 lists the calculated maximum stress increments and the strength utilization factors of the instrumented structural components within the four monitoring zones, that is, southeast zone, southwest zone, northeast zone, and northwest zone of the floating platform. From Table 1, it is seen that the maximum tensile stress increment during dismantlement of the temporary supports is 20.03 MPa with an SUF of 6.8%, happening at the structural component located at the southern web of the upper chord (the instrumented section number 2 as illustrated in Figure 4) of the main steel truss TR1 in the southeast zone of the floating platform, while the maximum compressive stress increment during dismantlement of the temporary supports is 21.42 MPa with an SUF of 7.3%, happening at the structural component located at the bottom flange of the bottom chord (the instrumented section number 4 as illustrated in Figure 4) of the main steel truss TR1 in the southeast zone of the floating platform. Both the maximum tensile stress increment and the maximum compressive stress increment during dismantlement of the temporary supports are much less than the allowable stress threshold which was set as 50 MPa.

Figure 10 illustrates the growth of stresses at the structural components at the instrumented sections number 2 and 4 of the floating platform in the temporary supports' dismantling process. In Figure 10, the location of a vibrating-wire strain gauge is denoted as "SXXNN-M," where XX represents the monitoring zone of the floating platform, for instance, SE stands for the sensors at the southeast zone of the floating platform; NN is the instrumented section; m is the sensor number. It is observed from Figure 10 that the stresses of the instrumented structural components (that are bisymmetrically distributed on the floating platform) grew step-by-step synchronously with the unloading process. With the help of the real-time SHM system, the temporary supports' dismantling duration was shortened to less than six hours from the originally scheduled three days.

5. Long-Term Strain Monitoring and Safety Evaluation

5.1. Long-Term Strain Monitoring Data. After the completion of dismantlement of the temporary supports, a variety of construction dead-loads such as glass curtain-walls, concrete floor-slabs, electromechanical facilities, and so forth were gradually applied on the floating platform. Real-time monitoring of the stress growth of key structural components of the floating platform is vital to guiding the massive construction in a well-organized manner in terms of both construction sequence and progress. The long-term SHM system for NHSSE has been continuously operating since the commencement of the unloading of the temporary supports of the floating platform.

In this study, two-year (from 3 April 2010 to 3 April 2012) strain monitoring data from all the installed vibrating-wire strain gauges have been acquired for statistical stress analysis and safety evaluation of the floating platform. Figure 11 illustrates the stress growth of the structural components at the instrumented sections number 2 and 4 of the floating platform in the two-year monitoring period

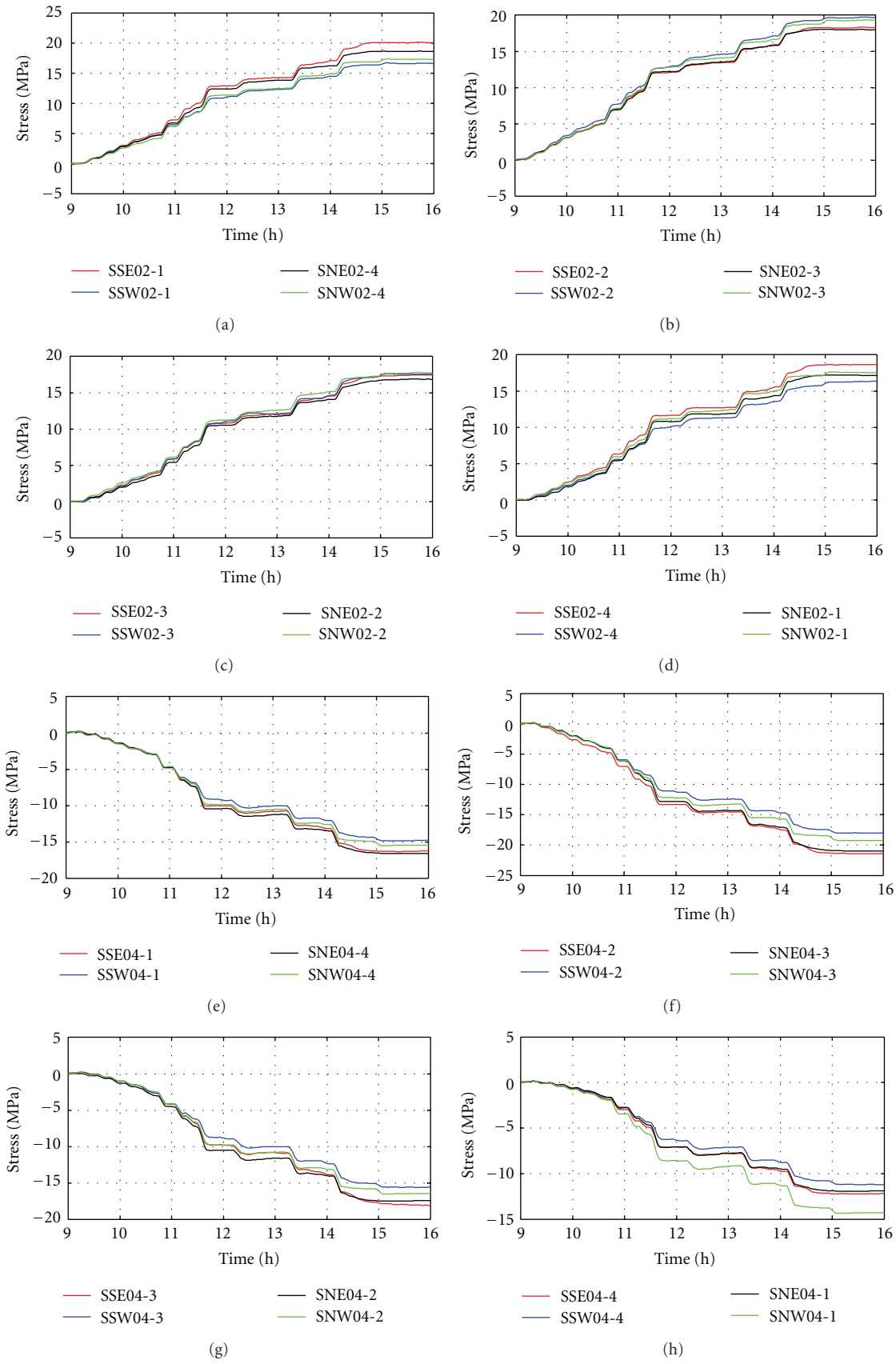

Figure 10: Growth of stresses during dismantlement of temporary supports.

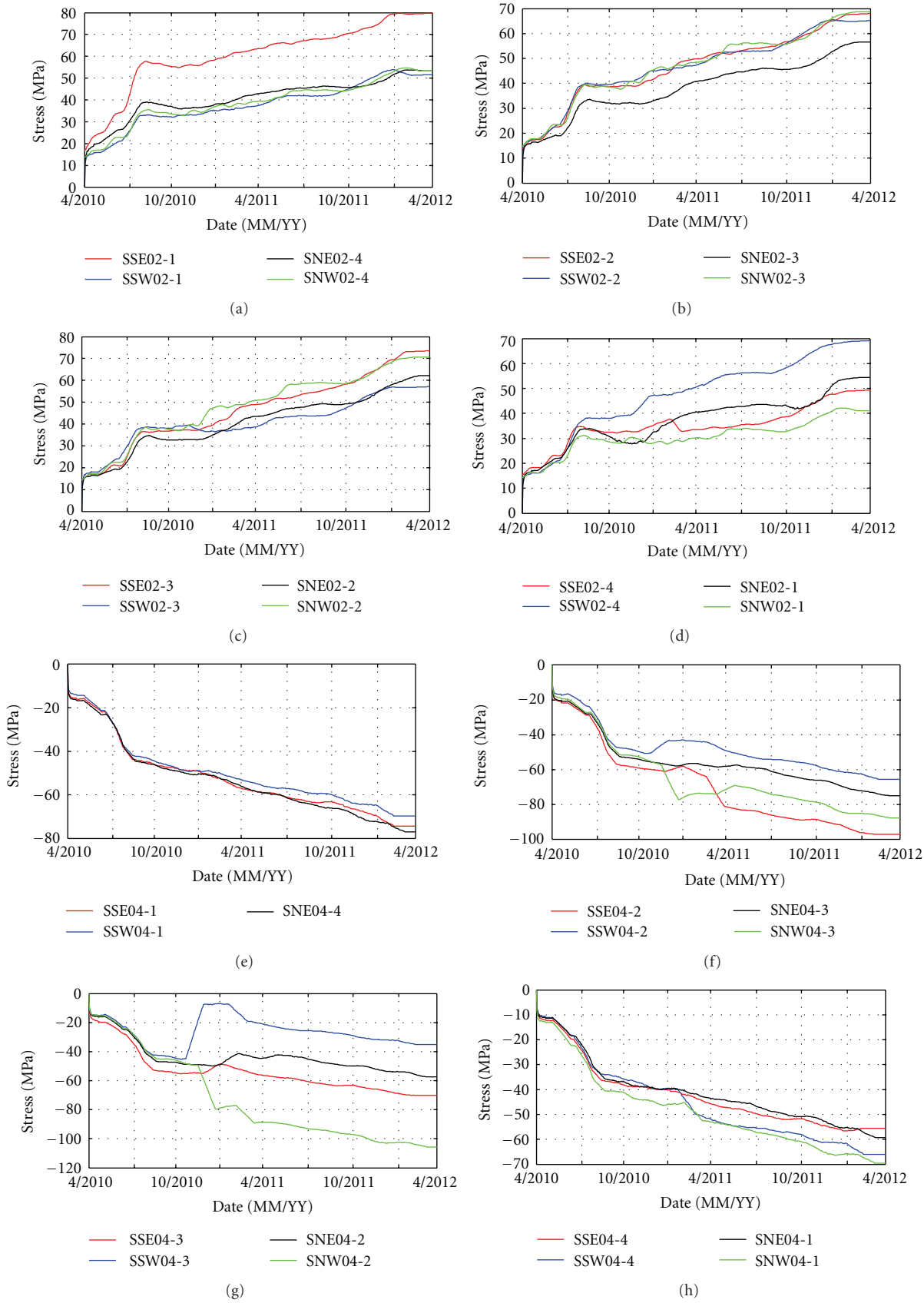

Figure 11: Two-year monitoring of structural stress growth.

Table 2: Statistics of the maximum stress increments and strength utilization factors after two-year monitoring.

Monitoring zone	Tensile stress increment (MPa)	SUF	Sensor location	Compressive stress increment (MPa)	SUF	Sensor location
Southeast (SE)	81.63	27.7%	2-1 (S)	71.66	24.3%	4–1 (S)
Southwest (SW)	69.45	23.5%	9–3 (N)	81.39	27.6%	7–4 (W)
Northeast (NE)	72.97	24.7%	9–1 (S)	74.40	25.2%	4-4 (N)
Northwest (NW)	73.98	25.1%	9–1 (S)	101.84	34.5%	4–2 (BS)

(the vibrating-wire strain gauge SNW04-4 was damaged in construction stage). It is seen from Figure 11 that the stresses of the bi-symmetrically distributed structural components are increased gradually and synchronously.

5.2. Statistical Analysis of Stress Increments. As listed in Table 2, the maximum stress increments and the strength utilization factors of the instrumented structural components within the four monitoring zones of the floating platform are derived by use of the two-year strain monitoring data. It is known from Table 2 that the maximum tensile stress increment after a two-year monitoring period is 81.63 MPa with an SUF of 27.7%. The structural component with the maximum tensile stress increment is located at the southern web of the upper chord (the instrumented section number 2 as illustrated in Figure 4) of the main steel truss TR1 in the southeast zone of the floating platform. The maximum compressive stress increment after a two-year monitoring period is 101.84 MPa with an SUF of 34.5%. The structural component with the maximum compressive stress increment is located at the bottom flange of the bottom chord (the instrumented section number 4 as illustrated in Figure 4) of the main steel truss TR1 in the northwest zone of the floating platform.

It appears from the data that both the maximum tensile stress increment and the maximum compressive stress increment after a two-year monitoring period are relatively low in comparison with the design strength. It is therefore concluded that the key structural components of the floating platform are safe with sufficient safety margins in recognition that the majority of the dead-loads of the floating platform have been imposed up to 3 April 2012. As illustrated in Figure 12, it was observed that the measured stress increment at the bottom flange of the bottom chord of the main steel truss TR1 in the northwest zone of the floating platform (monitored by the vibrating-wire strain gauge SNW04-2) on 2 December 2010 was −21.43 MPa, which is much larger than the stress increments at other three structural components bi-symmetrically distributed on the floating platform. After an in situ inspection, it was found that keel welding of the curtain-wall suspended ceiling was being executed adjacent to the vibrating-wire strain gauge SNW04-2 during that period of time, as shown in Figure 13.

5.3. Experiment on Welding Residual Stress. To identify the cause of the abrupt stress change of the above-mentioned structural component, a field experiment was conducted to investigate the features of the welding residual stress caused by the keel welding of the curtain-wall suspended ceiling.

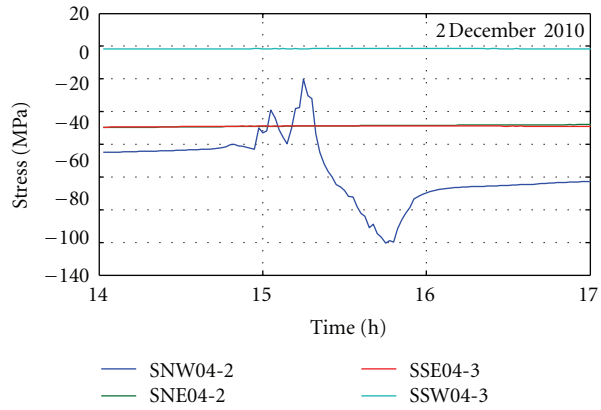

Figure 12: Stress increment pattern at welding-affected zone and other areas.

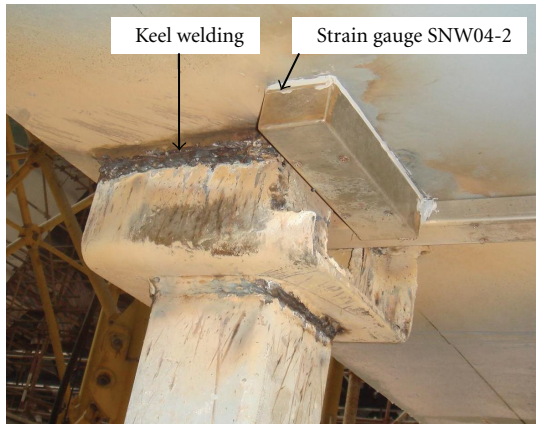

Figure 13: Keel welding of curtain-wall suspended ceiling.

The field welding experiment was carried out by welding the keel base onto the ceiling on the lower surface of the 7th floor of the floating platform with the same welding process as keel welding of the curtain-wall suspended ceiling. Seven vibrating-wire strain gauges capable of simultaneously measuring the strain and temperature were deployed around the keel base, and then the keel base was welded onto the ceiling following the prespecified welding process as illustrated in Figure 14. In Figure 14, SG-X and TEM-X are denoted as the strain and temperature sensors, respectively, in which X represents the sensor number. Figure 15 shows the welded keel base and the deployed strain gauges. It is worth underlining that the strain sensor SG-3, which is 50 mm away from the weld toe, was installed in accordance

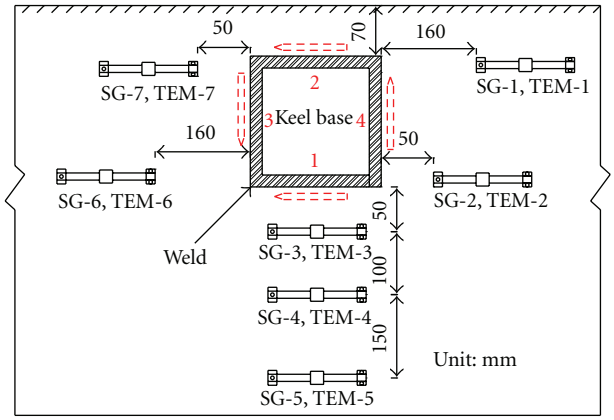

Figure 14: Deployment locations of strain gauges and welding process.

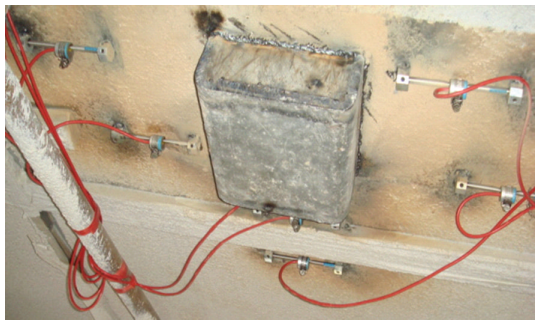

Figure 15: Photo of welded keel base and deployed strain gauges.

with the vibrating-wire strain gauge SNW04-2 in terms of the distance between the sensor and the weld toe as well as the sensor installation direction.

The welding process in this field experiment commenced at 13:26 pm on 14 April 2011 and ended at 14:22 pm on 14 April 2011. During the whole period of the welding experiment, the strain and temperature data were synchronously acquired from all the deployed sensors from 13:00 pm to 17:50 pm on 14 April 2011. Figure 16 shows the stress and temperature time histories of the seven deployment locations during the welding experiment. It is observed from Figure 16 that the stress variation is fairly complex during the welding process and becomes almost steady one hour after completion of welding. An insight into Figure 16 reveals that welding residual stresses are generated at the sensor deployment locations which can be derived by simply subtracting the initial value, which is treated as zero at the beginning of welding process, from the structural stress of each deployment location after the completion of welding.

Table 3 lists the evaluated welding residual stresses at the seven deployment locations by use of the strain monitoring data during the welding experiment. From Table 3, it is revealed that the welding residual stresses at the seven deployment locations vary dramatically in terms of the nature and amplitude of the welding residual stress. The

Table 3: Statistics of welding residual stress.

Strain sensor	Distance to weld toe (mm)	Welding residual stress (MPa)
SG-1	160	26.13
SG-2	50	15.24
SG-3	50	−23.12
SG-4	150	−5.30
SG-5	300	3.27
SG-6	160	7.37
SG-7	50	48.69

welding residual stress measured by the strain sensor SG-3 is −23.12 MPa, which is in line with the stress increment measured by the vibrating-wire strain gauge SNW04-2 on 2 December 2010 during the period of keel welding of the curtain-wall suspended ceiling. It is therefore concluded that the abrupt stress change of the vibrating-wire strain gauge SNW04-2 on 2 December 2010 was induced by the keel welding of the curtain-wall suspended ceiling.

6. Conclusions

In this paper, a long-term SHM system implemented on NHSSE featured by its huge floating platform has been outlined. This system was devised to monitor the health and safety condition of NHSSE in both construction and service stages. As part of this system, densely distributed strain sensor networks comprising 224 vibrating-wire strain gauges were constructed, from which strain monitoring data were real-time acquired and visualized remotely by forming a framework of local tethered data acquisition and long-range wireless data transmission. The effectiveness of the monitoring system was fully demonstrated in the process of dismantling the temporary supports for the floating platform during construction, through providing accurate real-time information on the evolution of structural stress which in turn greatly benefits the progress control and decision-making on the unloading procedure (the temporary supports' dismantlement duration was shortened to less than six hours from the originally scheduled three days).

Based on the statistical analysis of the real-time strain monitoring data acquired during and after dismantlement of the temporary supports of the floating platform, the following specific conclusions are obtained: (i) during dismantlement of the temporary supports, the stresses at the instrumented structural components bi-symmetrically distributed on the floating platform evolve in a step-by-step manner synchronously with the unloading process, and the stress increments of the structural components are much less than the allowable stress threshold; (ii) by examining two-year strain monitoring data from all the deployed sensors, it is revealed that the strength utilization factor of each instrumented structural component, which is defined as the ratio of the stress increment to the design strength of steel, is relatively low, indicating that the structural components of the floating platform are safe with sufficient safety margins;

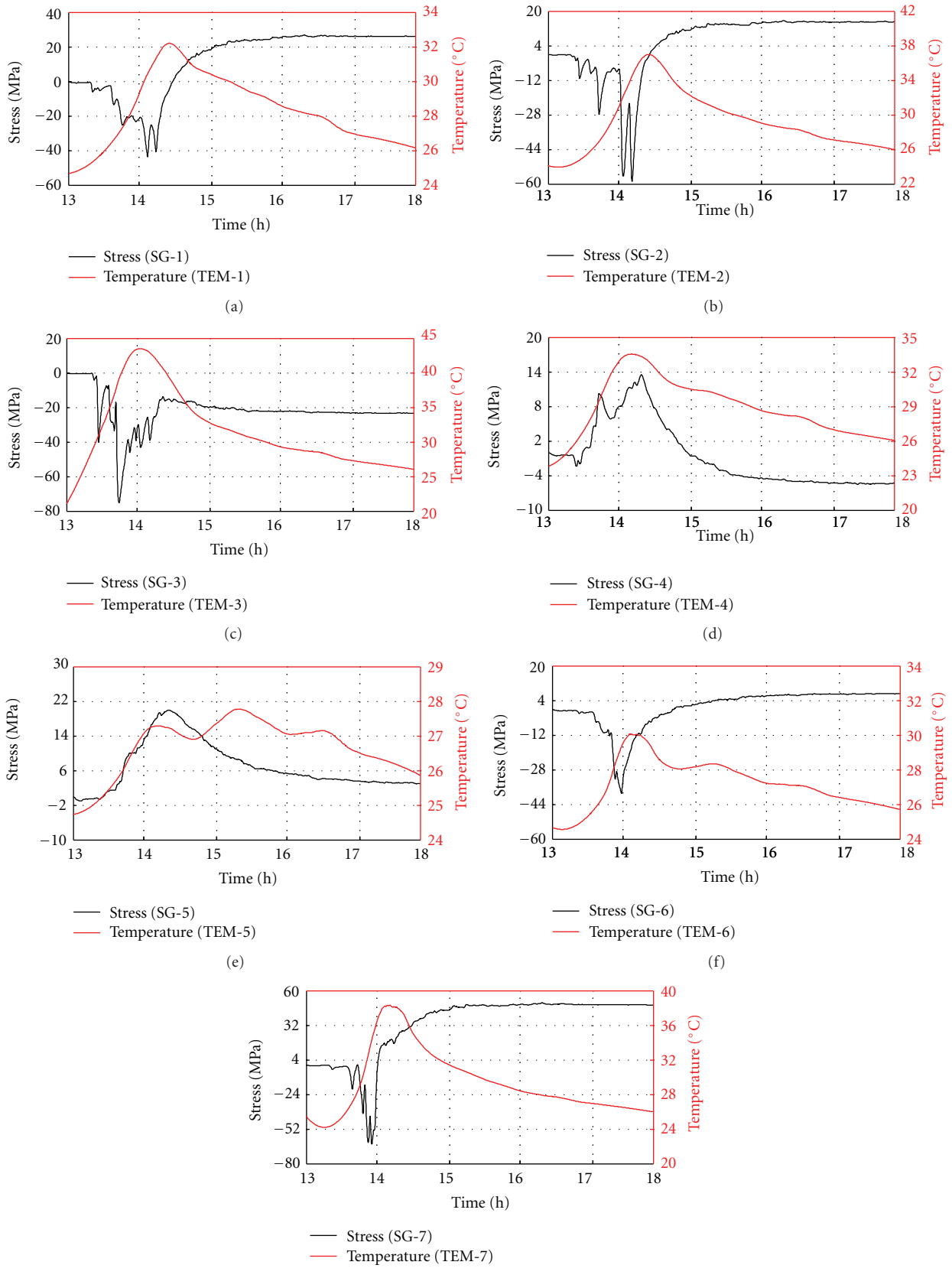

Figure 16: Stress and temperature time histories during welding.

(iii) the abrupt stress change of the deployed vibrating-wire strain gauge caused by the keel welding of the curtain-wall suspended ceiling is testified by the field welding experiment. The results of the field welding experiment reveal that the welding residual stresses at different sensor deployment locations vary dramatically in terms of the nature and amplitude of the welding residual stress.

Acknowledgments

The work described in this paper was supported by The Hong Kong Polytechnic University under the Grant G-U845 and through the Development of Niche Areas Programme (Project no. 1-BB68). The authors also wish to thank the engineers of Shenzhen Stock Exchange Operation Centre Management Co., Ltd. for their support throughout the work.

References

[1] R. D. Nayeri, S. F. Marsi, and A. G. Chassiakos, "Application of structural health monitoring techniques to track structural changes in a retrofitted building based on ambient vibration," *Journal of Engineering Mechanics*, vol. 133, no. 12, pp. 1311–1325, 2007.

[2] H. N. Li, T. H. Yi, X. D. Yi, and G. X. Wang, "Measurement and analysis of wind-induced response of tall building based on GPS technology," *Advances in Structural Engineering*, vol. 10, no. 1, pp. 83–93, 2007.

[3] A. Mita, H. Sato, and H. Kameda, "Platform for structural health monitoring of buildings utilizing smart sensors and advanced diagnosis tools," *Structural Control and Health Monitoring*, vol. 17, no. 7, pp. 795–807, 2010.

[4] T. H. Yi, H. N. Li, and M. Gu, "A new method for optimal selection of sensor location on a high-rise building using simplified finite element model," *Structural Engineering and Mechanics*, vol. 37, no. 6, pp. 671–684, 2011.

[5] T. H. Yi, H. N. Li, and M. Gu, "Recent research and applications of GPS-based monitoring technology for high-rise structures," *Structural Control and Health Monitoring*. In press.

[6] Y. Q. Ni, Y. Xia, W. Y. Liao, and J. M. Ko, "Technology innovation in developing the structural health monitoring system for Guangzhou New TV Tower," *Structural Control and Health Monitoring*, vol. 16, no. 1, pp. 73–98, 2009.

[7] Y. Q. Ni, K. Y. Wong, and Y. Xia, "Health checks through landmark bridges to sky-high structures," *Advances in Structural Engineering*, vol. 14, no. 1, pp. 103–119, 2011.

[8] T. H. Yi, H. N. Li, and M. Gu, "Optimal sensor placement for structural health monitoring based on multiple optimization strategies," *Structural Design of Tall and Special Buildings*, vol. 20, no. 7, pp. 881–900, 2011.

[9] W. H. Chen, Z. R. Lu, W. Lin et al., "Theoretical and experimental modal analysis of the Guangzhou New TV Tower," *Engineering Structures*, vol. 33, no. 12, pp. 3628–3646, 2011.

[10] P. L. Fuhr, D. R. Huston, P. J. Kajenski, and T. P. Ambrose, "Performance and health monitoring of the Stafford Medical Building using embedded sensors," *Smart Materials and Structures*, vol. 1, no. 1, pp. 63–68, 1992.

[11] A. J. Cardini and J. T. DeWolf, "Long-term structural health monitoring of a multi-girder steel composite bridge using strain data," *Structural Health Monitoring*, vol. 8, no. 1, pp. 47–58, 2009.

[12] H. Murayama, K. Kageyama, K. Uzawa, K. Ohara, and H. Igawa, "Strain monitoring of a single-lap joint with embedded fiber-optic distributed sensors," *Structural Health Monitoring*, vol. 11, no. 3, pp. 325–344, 2012.

[13] Y. Q. Ni, X. W. Ye, and J. M. Ko, "Monitoring-based fatigue reliability assessment of steel bridges: analytical model and application," *Journal of Structural Engineering*, vol. 136, no. 12, pp. 1563–1573, 2010.

[14] Y. Xia, Y. Q. Ni, P. Zhang, W. Y. Liao, and J. M. Ko, "Stress development of a supertall structure during construction: field monitoring and numerical analysis," *Computer-Aided Civil and Infrastructure Engineering*, vol. 26, no. 7, pp. 542–559, 2011.

[15] B. J. A. Costa and J. A. Figueiras, "Evaluation of a strain monitoring system for existing steel railway bridges," *Journal of Constructional Steel Research*, vol. 72, pp. 179–191, 2012.

[16] H. W. Xia, Y. Q. Ni, K. Y. Wong, and J. M. Ko, "Reliability-based condition assessment of in-service bridges using mixture distribution models," *Computers and Structures*, vol. 106-107, pp. 204–213, 2012.

[17] Y. Q. Ni, X. W. Ye, and J. M. Ko, "Modeling of stress spectrum using long-term monitoring data and finite mixture distributions," *Journal of Engineering Mechanics*, vol. 138, no. 2, pp. 175–183, 2012.

[18] X. W. Ye, Y. Q. Ni, K. Y. Wong, and J. M. Ko, "Statistical analysis of stress spectra for fatigue life assessment of steel bridges with structural health monitoring data," *Engineering Structures*, vol. 45, pp. 166–176, 2012.

[19] X. W. Ye, Y. Q. Ni, and J. M. Ko, "Experimental evaluation of stress concentration factor of welded steel bridge T-joints," *Journal of Constructional Steel Research*, vol. 70, pp. 78–85, 2012.

[20] Y. Q. Ni, Y. X. Xia, and X. W. Ye, "Structural health monitoring of a tall building with huge floating platform," in *Proceedings of the 4th International Conference on Smart Materials, Structures and Systems (Symposium G: Emboding Intelligence in Structures and Integrated Systems)*, Montecatini Terme, Italy, June 2012.